Classification of human grasp forces in activities of daily living using a deep neural network

Jesus Fernando Padilla-Magaña[1], Isahi Sanchez-Suarez[2], Esteban Peña-Pitarch[3]
[1]Department of Manufacturing Technologies, Polytechnic University of Uruapan, Michoacán, México
[2]Department of Physiotherapy, Polytechnic University of Uruapan, Michoacán, México
[3]Escola Politècnica Superior d'Enginyeria de Manresa (EPSEM), Polytechnic University of Catalonia (UPC), Barcelona, Spain

Article Info

Article history:

Received Jul 13, 2023
Revised Jun 24, 2024
Accepted Jun 26, 2024

Keywords:

Deep learning
Finger force
Force sensors
Human grasp
Rehabilitation

ABSTRACT

The study of human grasp forces is fundamental for the development of rehabilitation programs and the design of prosthetic hands in order to restore hand function. The purpose of this work was to classify multiple grasp types used in activities of daily living (ADLs) based on finger force data. For this purpose, we developed a deep neural network (DNN) model using finger forces obtained during the performance of six tests through a novelty force sensing resistor (FSR) glove system. A study was carried out with 25 healthy subjects (mean age: 35.4±11.6) all right handed. The DNN classifier showed high overall performance, obtaining an accuracy of 93.19%, a precision of 93.33%, and a F1-score of 91.23%. Therefore, the DNN classifier in combination with the FSR glove system is an important tool for physiotherapists and health professionals to determine and identify finger grasp forces patterns. The DNN model will facilitate the development of tailored and personalized rehabilitation programs for subjects recovering of hand injurie and other hand diseases. In future work, prosthetic hand devices can be optimized to more accurately reproduce natural grasping patterns.

Corresponding Author:

Jesus Fernando Padilla-Magaña
Department of Manufacturing Technologies, Polytechnic University of Uruapan Michoacán
1200 Uruapan-Carapan Highway, Uruapan, Michoacán 60210, México
Email: fe.padilla@upu.edu.mx

1. INTRODUCTION

The human hand is one of the most complex parts of the human body composed of 29 bones combined with an advanced muscular and ligamentous system which makes it difficult to study [1]. One of the main functions of the human hand is the object manipulation that allows the performance of several activities of daily living (ADLs). Grasping is an essential part of object manipulation as it enables the initial contact and control of the object. Once a proper grasp is achieved, the hand becomes capable of performing a wide range of manipulation actions, facilitating interaction with both the object and the environment. However, human grasping is a major challenge for people with prosthetic hands or who have suffered hand diseases or injuries. The current state of commercially available prosthetic hands is far from approaching human-level dexterity, even for relatively simple grasping activities [2]. The limited reliability, functionality and durability of prosthetic hands have resulted in low utilization or abandonment of sophisticated devices [3]. On the other hand, a typical consequence of traumatic brain injuries, degenerative brain diseases and strokes is a decreased ability to grasp and manipulate objects [4]. People with impaired hand function have a significantly lower quality of life because they are unable to perform ADLs, so the physical rehabilitation process is of utmost importance. Therefore, the study of human grasping is an important subject in biomechanics and medical rehabilitation, for the design of realistic prosthetic hands, the assessment of hand function and the development of specific rehabilitation programs [5]–[7]. In recent years, human hand motion (HHM) analysis has become an important tool for understanding human grasping. Several studies on HHM have been conducted in the areas of robotics, biomechanics, occupational therapy, neuroscience and artificial intelligence [8], [9]. HHM analysis uses several sensing technologies that provides information about hand position, force, and velocity over time for the development of computational models to study these motions [8]. Specifically, force information plays a vital role in the analysis of HHM, and particularly in the context of human grasping. One of the most widely used sensors for determining hand forces in HHM are the force sensing resistors (FSRs). The FSRs are robust polymer thick film (PTF) devices with piezoresistive sensing technology, which exhibit a reduction in resistance when force is exerted to their active area [10]. FSRs consist of a pair of split membranes with an adhesive layer that produces an air gap between them. One membrane is coated with a special resistive ink, while the other is printed with an interdigitated circuit composed of multiple electrically distinct traces. The value of the FSR sensor is inversely proportional to the applied force. When the sensor is pressed, the resistance of the FSR decreases as the force increases, due to the conductive ink within the sensor. Additionally, FSR sensors can measure both dynamic and static forces [11]. Recently, in order to measure and analysis human hand forces FSRs sensors have been used in several applications in medical rehabilitation and biomechanics [12]–[17]. Lately, the use of machine learning and deep learning (DL) algorithms using force data from FSRs, surface electromyography (sEMG), and force myography (FMG) sensors have been used to improve the accuracy rate for the detection and classification of Human grasp forces and motions. However, there has been limited research conducted in this area. Li *et al*. [18] measured pressure distribution patterns using an array of 32 FSR sensors placed around the forearm in combination with a support vector machine (SVM) algorithm for the classification of different finger motions including grasping motions. On the other hand, Wan *et al*. [19] classify 21 distinct hand gestures developing a k-nearest neighbor (kNN) classification algorithm using forearm electromyography (EMG) signals acquired with a Myo armband and muscle pressure signals from the back of the hand acquired with an array of five FSRs. Kakoty and Hazarika [20] used an SVM algorithm based on a radial basis function (RBF) with forearm EMG signals to classify six different grasp types used during daily living activities. Coskun *et al*. [21] proposed a convolutional neural network model (1D-CNN) to classify six grasp types using as features surface EMG and sEMG signals. Jiang *et al*. [22] classified different types of grasping by a linear discriminant analysis (LDA) model using an FMG system composed of an array of 16 FSR sensors placed on the wrist. Therefore, in this study we propose the use of a deep neural networks (DNNs) model for multiclass classification using fingertip force as features unlike previous studies that have been focused in forearm muscle force. Although traditional machine learning classification algorithms, such as SVM, random forest (RF), and kNN, have been successfully used in clinical applications. In addition, DNNs have significant advantages in transforming low-level features into complex high-level features across neurons and thus learning more complex and nonlinear patterns [23], [24]. The aim of this work was to classify several grasp types used in ADLs based on finger force data. Therefore, we presented the development of a low-cost and novelty FSR glove system for finger forces measurement. The force system was evaluated during the performance of six test that involves several grasps used in ADLs in healthy subjects. Subsequently, the dataset obtained was used for the development of a DNN model for the classification of the six grasp types using as features the force data obtained with the FSR glove system. This study contributes to the development of a novel high-performance DNN model capable of recognizing and classifying finger force patterns associated with different types of grasping used in ADLs. These advances offer significant advantages for the design of prosthetic hands and rehabilitation programs tailored to subjects with upper extremity impairments.

2. MATERIALS AND METHODS

2.1. The proposed FSR glove system

The design of the FSR Glove systems is described in this section. The FSRs were placed at the distal segments of the fingers because the purpose of the system was to study the force exerted on the fingertips during the grasping of different items in diverse activities. Therefore, based on size and the functional characteristics of the sensor, the FSR 07 model (Ohmite Manufacturing Company, USA) was chosen. Model FSR 07 has the following features: a thickness of 0.375 mm (including adhesive), an active area of 14.7 mm and a sensor overall length of 56.34 mm and overall width of 18.0 mm.

2.1.2. Signal conditioning

At this phase, a sensor conditioning circuit was built to generate a variable voltage as a function of the force applied on the sensor. Common conditioning methods include using a voltage divider and the inverting operational amplifier (op-amp) circuit. However, several studies [25]–[27] have demonstrated that inverting op-amp circuits with FSRs exhibit linear behavior between voltage and pressure at both low and high values. Since the study activities included objects of various sizes and the range of pressures would be different in each fingertip, we decided to use an inverting op-amp for signal conditioning. In this configuration, the output voltage (VOUT) exhibits an opposite polarity to the reference voltage (VREF). Furthermore, as the resistance of the FSR (RFSR) increases, the VOUT decreases proportionally. Consequently, when no pressure is applied in this configuration, the circuit generates zero VOUT as a result of the high RFSR impedance [28]. Nonetheless, VOUT increases as force is exerted, either significantly or minimally, based on the resistor value (RG) selected. In (1) delineates the amplifier's output.

$$\mathrm{Vout} = -\frac{\mathrm{R_G}}{\mathrm{R_{FSR}}} \cdot \mathrm{V_{REF}} \tag{1}$$

The inverting op-amp configuration included a combination of a voltage regulator, an op-amp, and a resistor. We chose the LM324 quad op-amp device for its cost-effectiveness and low voltage requirements. Subsequently, the appropriate RG was determined taking into account the following considerations. Since the microcontroller are limited to a power input of 5 V, exceeding this voltage would cause saturation and render the circuit unusable. Additionally, the highest fingertip strength applied on the FSRs was determined with a multimeter, reaching an RFSR value of 100 Ω. Therefore, a RG of 150 Ω was selected to ensure a VOUT close to 5 V. Finally, we use a first-order active low-pass filter for attenuating high-frequency interference. A cutoff frequency of 60 Hz was considered adequate for reducing the signal interference from the electrical circuit. For this purpose, a 22 µF capacitor was used.

2.1.3. Calibration

Finally, FSR sensors underwent static calibration prior to application to minimize inaccuracies; multiple studies have used comparable calibration procedures [14], [29], [30]. Throughout the test, the VOUT was recorded using the parallax data acquisition tool (PLX-DAQ) application. Next, calibrated weights of different magnitudes were then mounted on each FSR for generating a plot of the relationship of the exerted force to the VOUT, which resulted in the calibration curve equations. The results indicate that the VOUT increases proportionally to the amount of force applied. In addition, the derived equations offer the possibility to extend the findings to higher pressures as needed. Coefficients of correlation and calibration equations are shown in Table 1.

Once the FSR signals were conditioned, we proceed to the data acquisition phase. The transformation from analog to digital signals followed these steps: the inverter op-amp output pins were connected to the analog ports of an Arduino Nano to transform the analog voltage using a 10-bit analog-to-digital converter (ADC). Next, using the equations found during the calibration process, we created a sketch to read the analog inputs of each FSR sensor and convert them into force values. Once the force values were acquired, they were transferred wirelessly to a user friendly graphic user interface created in unity v.2020.2.1. The HC-05 (bluetooth module) was used for this purpose, employing the serial port protocol (SPP). Sensor data obtained during each of the tests were collected at a frequency of 50 Hz and stored in a file of comma-separated values (CSV). Next, the data was filtered with a 5-Hz low-pass second order Butterworth filter, similar to previous studies of HHM analysis [31]–[34]. Finally, the FSR sensors were mounted in a flexible glove on the distal segments of the fingers.

Table 1. Calibration equations for FSR sensors

Sensor	Calibration equation	Coefficient of correlation ($\mathcal{R}^2$)
1	$3.6915x - 0.2895$	0.994
2	$3.6497x - 0.3745$	0.991
3	$3.7318x - 0.6047$	0.992
4	$3.7741x - 0.6082$	0.994
5	$3.7543x - 0.3652$	0.990

2.2. Participants

Twenty-five healthy individuals participated in this study, 13 women and 12 men (mean age: 35.4±11.6, hand length (HL): 186.7 cm±13.1 cm, hand breadth (HB): 83.1 cm±7.6 cm). The inclusion criteria include the following requirements: right-handed, being at least 18 years old, having no history of hand disorders or injuries, and reported to be 100% functional with the right hand. The study was performed with the approval of the Ethics Committee of the Universidad Politécnica de Uruapan (UPUCE/F004/2022) and all subjects signed an informed consent for inclusion after being informed of the protocol which was in accordance with the declaration of Helsinki.

2.3. Experimental setup

The study was conducted at the Universidad Politécnica de Uruapan facilities. The HL and HB were determined in each subject using a measuring tape. Participants were fitted with the FSR glove on the right-hand, the force system was mounted on the wrist with a velcro strap, and bluetooth communication with the user interface was tested (Figure 1). Participants were then instructed to hold, grasp, and lift each item using the wearable device. Each participant performed the six tests three times each. Six items commonly used in ADLs were selected for testing in this study. The items varied in size, weight, and shape, requiring different grasping configurations and forces during each test. The grasp types used during each test were classified according Cutkosky's grasp taxonomy [35]. The characteristics of the objects and the grasp classification are shown in Table 2. The force data was determined and stored in a CSV file throughout the entire duration of each test for further statistical analysis. At the beginning of each trial, the hand was placed horizontally on a table in a neutral position. Next, in the pre-grasp phase, no force was exerted on the object; therefore, it was not taken into consideration in the analysis. Then, during the grasping phase, the maximum force is reached when the object is lifted. Finally, as the participant drops the item, the force gradually decreases and the fingers return to their initial position. As a result, the peak force values from the three trials performed on each subject were averaged for each task. We identified these averaged values as the subject's maximum finger force during a task. The maximum finger forces of all 25 subjects were then averaged.

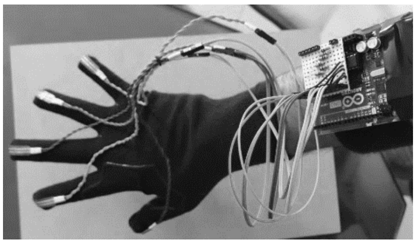

Figure 1. A participant wearing the FSR glove system

Table 2. Objects description and grasp classification of each test

Test	Item	Size	Weight (g)	Grasp type
1	Wooden block	10 cm^3	490	Large diameter heavy wrap
2	Wooden block	7 cm^3	195	Medium wrap
3	Wooden block	2.5 cm^3	6.5	Tripod grasp
4	Tennis ball	Diameter, 6.7 cm	60	Sphere precision grasp
5	Marble	Diameter, 1.8 cm	5.4	Thumb+1 finger pinch
6	Plastic tumbler with water	Diameter, 7 cm	320	Sphere power grasp

2.4. Deep neural network

DL is a subfield of machine learning, which is based essentially in artificial neural networks (ANNs). In turn, an ANN is a computer model inspired on the flow of data processed throughout neurons in the human brain [36]. The structure of an ANN is represented as a set of layers, which are defined as input, hidden and output layers. The neurons in the input layer corresponds to the number of features in the dataset and passes them to the rest of the network. The hidden layers are intermediate layers between the input and output layers and process the data. Finally, the number of neurons in the output layer is the same as the corresponding outputs connected to each input, and these neurons produce the final results. However, when an ANN has multiple hidden layers between the input and output layers, this is defined as DNNs. DNNs are often employed for their ability to model complex non-linear relationships accurately and adaptively in classification tasks [24], [37].

2.4.1. Data preprocessing

The DNN model were developed in Anaconda (Anaconda Inc., TX, USA). Once the force data were collected with the FSR glove system, we started the process to data pre-processing. Importantly, in the DNN classifier we used the three maximum force values obtained for each subject during each of the six tests so a total of 450 samples composed the dataset. Initially, we distinguish input and output variables within the data set, commonly referred to as features and responses, respectively. In contrast, the response variables were the classes corresponded to the grasp type, so the model has six outputs labeled. The dataset has 11 inputs also known as features, that includes demographic characteristics as age, gender, HB, and HL. In addition, the weight of each object and the force values of each finger were also considered as features of the model. Next, the categorical feature (gender) was was then converted to binary multidimensional vectors through the one-hot encoding technique. The classes in the dataset were balanced with 25 samples in each class and no missing values were found, so the 450 samples were employed in the DNN. Subsequently, the DNN's overall performance was evaluated using two validation methods. First, we use the hold-out method, in which data set is divided into two parts: a training set and a test set. Therefore, we used 75% of the data as training set and the remaining 25% as test set. In addition, we used k-fold cross-validation (CV) method. This method enables us to evaluate and test the performance of our model in predict data on the test set (unseen data). The k-fold CV method is a follows the data sample is split into k equal number of folds. Then, the model used k-1 of the folds as training set and the remaining fold as the test set; this process is repeated k times, using each fold as a test set only once. During each iteration, a performance measure is computed e.g. accuracy. Therefore, the performance metric obtained using k-fold CV is the mean obtained during all interactions.

2.4.2. Deep neural network configuration

The DNN classifier has five layers which are the input layer, three hidden layers, and the output layer composed as follows. The input layer was defined according to the features in the dataset therefore 11 inputs were used. In addition, three hidden layers were used with the "rectified linear unit" (relu) funtion with 30 neurons each. Furthermore, this is a multi-class classification problem with six outputs, therefore six neurons were used in the output layer using the activation function (softmax). In the DNN we used the dropout technique, which is a powerful method to prevent overfitting and efficiently combine a wide range of neural networks architectures [38]. Therefore, a dropout rate of 20% was used from the input layer to the first hidden layer. Subsequently, GridSearchCV (GSCV) technique was applied to the DNN classification model to find the optimal performance of the model. Hyperparameters are adjustable parameters which values define the model performance and are set before the model training process. One of the most commonly used computational methods to find the optimal hyperparameters is the GSCV technique. This method analyzes every possible combination of parameter values of a given model using k-fold cross validation. Finally, the following metrics were used for evaluate the multi-class classification model: accuracy, precision, recall and F1-score. In addition, unlike the accuracy metric, which is calculated in the same way as in a binary classifier, the other metrics of the multiclass classification are calculated as the arithmetic mean of the individual class metrics [39]. The formulas of the evaluation metrics are shown in Table 3.

Table 3. Formulas of multi-class evaluation metrics

Metric	Formula
Accuracy	$\frac{TP+TN}{TP+FP+TN+FN}$
Precision	$\frac{\sum_{k=1}^{K} Precision_k}{K}$
Recall	$\frac{\sum_{k=1}^{K} Recall_k}{K}$
F1-score	$2 \times \frac{Macro\ Averaged\ Precision \times Macro\ Averaged\ Recall}{Macro\ Averaged\ Precision^{-1} \times Macro\ Averaged\ Recall^{1}}$

3. RESULTS AND DISCUSSION

3.1. Fingertip forces

In this section, we discussed the results obtained with the FSR glove system. The mean maximum finger forces obtained from performing the six tests are shown in Table 4. Test 1, which used a large diameter heavy grasp, showed the highest forces in all five digits (thumb 6.2 N, index 3.32 N, middle 4.4 N, ring 3.04 N, and little 1.85 N). In contrast, similar forces were used in the tests 2 and 6 in the fingers thumb, index, middle, and ring, as is shown in Figure 2. On the other hand, test 3 (thumb 2.68 N, index 2.43, and middle 1.60 N) and test 5 (thumb 1.83 N and index 1.46 N) showed the lower forces. In addition, the results demonstrated that the maximum total force of 18.81 N was applied during the performance of the large diameter heavy wrap grasp. In this test a power grasp was executed, this grasp is used when it is necessary to hold an object with an important force and it is executed between the fingers and the palm of the hand. Furthermore, the fingers flex more, employing flexion at all finger joints and the thumb acting as a buttress [40]. In contrast, the results showed that the minimum total finger force was found during the performance of the thumb+1 finger pinch (4.38 N) and the sphere precision grasp (6.71 N). In these tests, a precision grasp was executed using the terminal pads of the thumb and one or more of the rest fingers [41]. The precision grasp involves the execution of delicate and precise movements, requiring the use of less force [42]. On the other hand, the finger force distribution during each test using different grasp types is shown in Figure 2. The finger force distribution allows to know the number of fingers used at the moment of grasping an object and thus classify the type of grasping performed. In addition, we observed a relationship between the number of fingers used and the object's size, similar results were found in other studies [43], [44].

Table 4. Descriptive statistics of fingertip forces during the performance of the six tests

Test	Grasp type	Thumb (N)		Index (N)		Middle (N)		Ring (N)		Little (N)	
		Mean	SD	Mean	SD	Mean	SD	Mean	SD	Mean	SD
1	GT_1	6.20	2.19	3.32	1.79	4.40	1.92	3.04	1.75	1.85	0.99
2	GT_2	4.38	2.16	1.99	1.89	2.14	1.12	1.35	1.02	0.03	0.11
3	GT_3	2.68	1.64	2.43	1.23	1.60	1.20	0.18	0.42	0.01	0.04
4	GT_4	3.80	2.02	1.64	1.49	2.11	0.79	1.05	0.77	0.05	0.18
5	GT_5	1.83	1.26	2.45	1.53	0.01	0.04	0.12	0.25	0.02	0.08
6	GT_6	4.43	2.07	1.46	1.05	2.56	1.07	1.09	0.89	0.12	0.26

N=force in newtons; GT_1=large diameter heavy wrap; GT_2=medium wrap; GT_3=thumb+1 finger pinch; GT_4=sphere power grasp; GT_5=sphere precision grasp; GT_6=tripod grasp; and SD=standard deviation

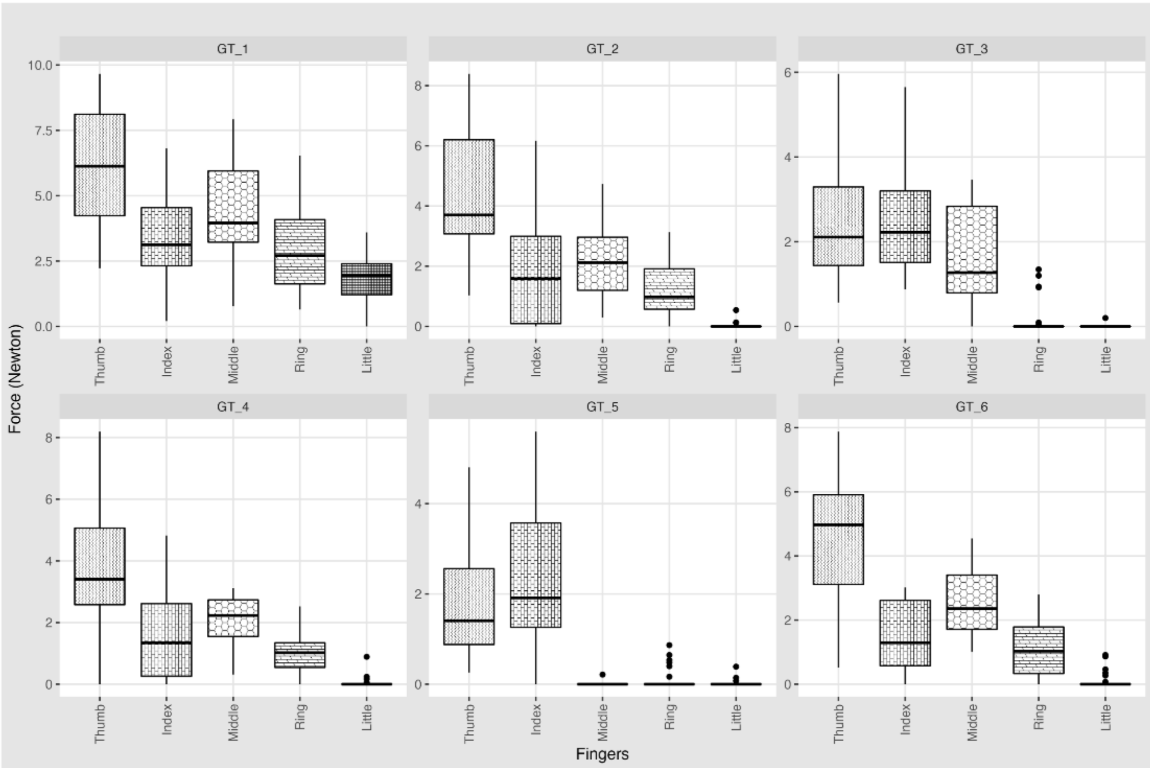

Figure 2. Boxplots of the maximum force values of all the fingers during each test

3.2. Deep neural network model

This section presents the results obtained from a DNN model used to classify a set of six different grasp types commonly used in ADLs. The model utilizes force data collected with the FSR glove system as features. The classifier was implemented in the following environment, operating system: macOS Sonoma 14, central processing units (CPU): Intel Core i7 (2.6 GHz), and memory: 16 GB RAM.

3.2.1. Hyperparameters selection

In order to obtain the best classifier performance, GSCV technique was applied to the DNN model using a five k-fold CV. GSCV has proven to be efficient in numerous clinical investigations where machine learning classification models were implemented [45], [46]. The hyperparameter values obtained were as: DNN ['batch_size': 32, 'epochs': 150, and 'optimizer': 'RMSprop'].

3.2.2. Deep neural network performance in the test set

The best performing hyperparameters obtained were employed to evaluate the DNN classifier performance in predicting results on the testing set. Table 5 presents the classification report with several evaluation metrics for the DNN model. The results of the DNN classifier showed a 100% of precision, recall, and F1-score in the classes GT_1, GT_2, GT_4, and GT_6. In contrast, the classes GT_3 and GT_5 showed a lower precision (92% and 83%), recall (80% and 94%), and F1-score (86% and 88%), respectively. On the other hand, the overall performance of the DNN classifier in the test set was similar in precision weighted, recall weighted, F1-score weighted and accuracy achieving a 96%. On the other hand, the confusion matrix in Figure 3 shows excellent performance in classifying the GT_1, GT_2, GT_4, and GT_6 classes. On the other hand, the classification of class GT_3 showed a good performance because 10 % of the samples were categorized as GT_5 class. In contrast, the classification of class GT_5 showed a regular performance because 20% of the samples were categorized as GT_3 class.

Table 5. DNN classification report

Evaluation metrics	Class	Precision	Recall	F1-score
	GT_1	1.00	1.00	1.00
	GT_2	1.00	1.00	1.00
	GT_3	0.92	0.80	0.86
	GT_4	1.00	1.00	1.00
	GT_5	0.83	0.94	0.88
	GT_6	1.00	1.00	1.00
Accuracy				0.96
Macro avg		0.96	0.96	0.96
Weighted avg		0.96	0.96	0.96

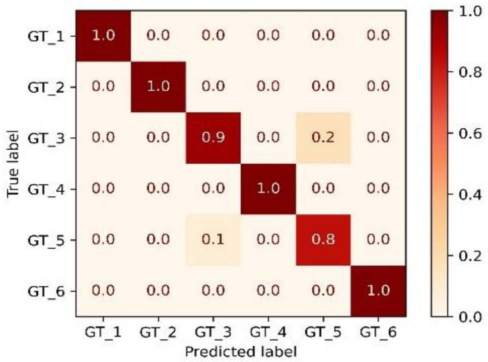

Figure 3. DNN model confusion matrix

3.2.3. Cross validation

Finally, five k-fold CV was implemented for evaluate and validate the overall performance of the DNN model. The average values and standard deviation obtained in several multi-class evaluation metrics are shown in Table 6. The DNN model showed an excellent performance in several metrics, achieving an accuracy of 93.19%, precision of 93.33% and a F1-score weighted of 91.23%. Coskun *et al*. [21] presented similar results using DL methods obtaining an accuracy of 94.94% in the classification of six hand movements. In contrast, Jiang *et al*. [22] used a LDA to classify 16 different grasps achieving an average accuracy of 82%. However, each of the studies used different types of sensors and information for the development of the classification models. In our study we used FSRs data. In contrast, Coskun *et al*. [21] used as features sEMG signals obtained of two forearm electrodes, while Jiang *et al*. [22] used FMG data. Therefore, each of the sensors used in these studies measured different types of force. In our study, we used FSR sensors to measure the pressure or normal force applied to the sensing element. In contrast, sEMG sensors records electrical activity during muscle contractions using surface electrodes, while FMG relies on FSR sensors placed on the skin or integrated into wearable devices to detect volumetric changes in the underlying muscles during contractions and movements [47]. However, the DNN model demonstrated a lower precision in the classification of the thumb+1 finger pinch and sphere precision grasp as is shown in the classification report in Table 5. We consider that the accuracy is lower during the performance of these tasks due to the maximum forces in the thumb and index fingertips were similar in the two tests as is shown in Table 4 and Figure 2. Therefore, the results obtained demonstrate that utilizing DNNs for human grasp classification based on finger forces may offer significant advantages for future work in prosthetic hand design and the implementation of personalized rehabilitation procedures. Prosthetic devices can be improved to replicate accurately natural grasp patterns, which will improve the user experience by providing users with greater comfort, functionality, and confidence in performing ADLs. In addition, identify and classified finger force patterns during the performance of several types of grasping, rehabilitation programs can be tailored to individual needs. Physiotherapy can use this information to develop interventions aimed at improving specific grasping functions based on each person's abilities and difficulties.

Table 6. Results of the evaluation metrics using a five-fold cross validation

Metric	Mean (%)	SD (%)
Accuracy	93.19	1.9
Precision weighted	93.33	1.7
Recall weighted	92.31	3.2
F1-score weighted	91.23	2.4

3.3. Limitations

Nevertheless, the present work had some limitations. We were restricted to using five FSR sensors due to the analog inputs of the Arduino board utilized. Therefore, we believe that for future research, it would be imperative to incorporate a data acquisition board to expand the number of available analog inputs, thus enabling a more complete analysis of the hand. On the other hand, only FSRs sensors were used in this study, however FMG or sEMG sensors could be included in future research. Using sEMG sensors to capture the electrical signals from the muscles, along with FMG sensors to detect the actual muscle contractions, can enhance the feature representation of DL models. Therefore, combining these signals with data on finger forces obtained with FSRs could improve the classification accuracy and robustness of the models. Finally, future research would benefit from the incorporation of a motion capture system using data gloves or inertial measurement units (IMUs), as proven in other studies [32], [48], [49].

4. CONCLUSION

The DNN demonstrates high performance in classifying and evaluating finger force patterns during the execution of various grasping tasks commonly used in ADLs, achieving an accuracy of 93.19%. In addition, the model can provide real-time feedback to patients, helping them to achieve correct grasping patterns and improve their motor skills through specific rehabilitation programs. Therefore, the combination of the DNN classifier and the FSR glove system is an important tool for health professionals. On the other hand, the DNN model proposed is useful in other areas as robotics and prosthetics. Using the DNN model in robotics to determine the appropriate grasp type based on the object characteristics as well as to determine the distribution and magnitude of finger forces necessary during object manipulation. In contrast, prosthetic hands technology will enable more precise emulation of natural hand movements, thereby further enhancing the quality of life for individuals using prosthetic devices.

ACKNOWLEDGMENTS

The authors acknowledge the Polytechnic University of Uruapan, Michoacán for providing the facilities for this study and extend their gratitude to all the participants involved. This research was partially supported by the National Council of Humanities, Sciences and Technologies (CONAHCYT) of Mexico, grant number A1-S-44382 of CB2017-2018.

REFERENCES

[1] Ł. Jaworski and R. Karpiński, "Biomechanics of the human hand," *Journal of Technology and Exploitation in Mechanical Engineering*, vol. 3, no. 1, pp. 28–33, Jun. 2017, doi: 10.35784/jteme.536.

[2] F. Cordella *et al.*, "Literature review on needs of upper limb prosthesis users," *Frontiers in Neuroscience*, vol. 10, May 2016, doi: 10.3389/fnins.2016.00209.

[3] Q. Fu and M. Santello, "Improving fine control of grasping force during hand-object interactions for a soft synergy-inspired myoelectric prosthetic hand," *Frontiers in Neurorobotics*, vol. 11, Jan. 2018, doi: 10.3389/fnbot.2017.00071.

[4] M. Nilsson, J. Ingvast, J. Wikander, and H. Von Holst, "The soft extra muscle system for improving the grasping capability in neurological rehabilitation," in *2012 IEEE-EMBS Conference on Biomedical Engineering and Sciences,* Dec. 2012, pp. 412–417, doi: 10.1109/IECBES.2012.6498090.

[5] B. Abbasi, E. Noohi, S. Parastegari, and M. Zefran, "Grasp taxonomy based on force distribution," in *25th IEEE International Symposium on Robot and Human Interactive Communication,* Aug. 2016, pp. 1098–1103, doi: 10.1109/ROMAN.2016.7745245.

[6] T. Feix, J. Romero, H. B. Schmiedmayer, A. M. Dollar, and D. Kragic, "The GRASP taxonomy of human grasp types," *IEEE Transactions on Human-Machine Systems*, vol. 46, no. 1, pp. 66–77, Feb. 2016, doi: 10.1109/THMS.2015.2470657.

[7] A. García Álvarez, A. Roby-Brami, J. Robertson, and N. Roche, "Functional classification of grasp strategies used by hemiplegic patients," *PLoS ONE*, vol. 12, no. 11, p. e0187608, Nov. 2017, doi: 10.1371/journal.pone.0187608.

[8] Z. Ju and H. Liu, "Human hand motion analysis with multisensory information," *IEEE/ASME Transactions on Mechatronics*, vol. 19, no. 2, pp. 456–466, Apr. 2014, doi: 10.1109/TMECH.2013.2240312.

[9] Y. Xue, Z. Ju, K. Xiang, J. Chen, and H. Liu, "Multimodal human hand motion sensing and analysis-a review," *IEEE Transactions on Cognitive and Developmental Systems*, vol. 11, no. 2, pp. 162–175, Jun. 2019, doi: 10.1109/TCDS.2018.2800167.

[10] C. Guo, C. Wu, B. Wang, and H. Liu, "A two-dimensional deflection sensor based on force sensing resistors," *Journal of Sensors*, vol. 2017, pp. 1–8, 2017, doi: 10.1155/2017/1241280.

[11] A. S. Sadun, J. Jalani, and J. A. Sukor, "Force sensing resistor (FSR): a brief overview and the low-cost sensor for active compliance control," in *First International Workshop on Pattern Recognition*, , vol. 10011, p. 1001112 Jul. 2016, doi: 10.1117/12.2242950.

[12] H. Liu *et al.*, "A glove-based system for studying hand-object manipulation via joint pose and force sensing," in *IEEE International Conference on Intelligent Robots and Systems*, Sep. 2017, vol. 2017, pp. 6617–6624, doi: 10.1109/IROS.2017.8206575.

[13] A. Nikonovas, A. J. L. Harrison, S. Hoult, and D. Sammut, "The application of force-sensing resistor sensors for measuring forces developed by the human hand," *Proceedings of the Institution of Mechanical Engineers, Part H: Journal of Engineering in Medicine*, vol. 218, no. 2, pp. 121–126, Feb. 2004, doi: 10.1243/095441104322984013.

[14] Q. Ye, M. Seyedi, Z. Cai, and D. T. H. Lai, "Force-sensing glove system for measurement of hand forces during motorbike riding," *International Journal of Distributed Sensor Networks*, vol. 2015, no. 11, p. 545643, Nov. 2015, doi: 10.1155/2015/545643.

[15] E. Battaglia *et al.*, "ThimbleSense: a fingertip-wearable tactile sensor for grasp analysis," *IEEE Transactions on Haptics*, vol. 9, no. 1, pp. 121–133, Jan. 2016, doi: 10.1109/TOH.2015.2482478.

[16] S. Ganeson, R. Ambar, and M. M. A. Jamil, "Design of a low-cost instrumented glove for hand rehabilitation monitoring system," in *Proceedings-6th IEEE International Conference on Control System, Computing and Engineering*, 2017, pp. 189–192, doi: 10.1109/ICCSCE.2016.7893569.

[17] M. Hoda, Y. Hoda, B. Hafidh, and A. El Saddik, "Predicting muscle forces measurements from kinematics data using kinect in stroke rehabilitation," *Multimedia Tools and Applications*, vol. 77, no. 2, pp. 1885–1903, Jan. 2018, doi: 10.1007/s11042-016-4274-5.

[18] N. Li, D. Yang, L. Jiang, H. Liu, and H. Cai, "Combined use of FSR sensor array and SVM classifier for finger motion recognition based on pressure distribution map," *Journal of Bionic Engineering*, vol. 9, no. 1, pp. 39–47, Mar. 2012, doi: 10.1016/S1672-6529(11)60095-4.

[19] B. Wan, R. Wu, K. Zhang, and L. Liu, "A new subtle hand gestures recognition algorithm based on EMG and FSR," in *Proceedings of the 2017 IEEE 21st International Conference on Computer Supported Cooperative Work in Design*, Apr. 2017, pp. 127–132, doi: 10.1109/CSCWD.2017.8066682.

[20] N. M. Kakoty and S. M. Hazarika, "Recognition of grasp types through principal components of DWT based EMG features," in *IEEE International Conference on Rehabilitation Robotics*, Jun. 2011, pp. 1–6, doi: 10.1109/ICORR.2011.5975398.

[21] M. Coskun, O. Yildirim, Y. Demir, and U. R. Acharya, "Efficient deep neural network model for classification of grasp types using sEMG signals," *Journal of Ambient Intelligence and Humanized Computing*, vol. 13, no. 9, pp. 4437–4450, Sep. 2022, doi: 10.1007/s12652-021-03284-9.

[22] X. Jiang, L. K. Merhi, and C. Menon, "Force exertion affects grasp classification using force myography," *IEEE Transactions on Human-Machine Systems*, vol. 48, no. 2, pp. 219–226, Apr. 2018, doi: 10.1109/THMS.2017.2693245.

[23] X. Y. Liu, Y. Fang, L. Yang, Z. Li, and A. Walid, "High-performance tensor decompositions for compressing and accelerating deep neural networks," in *Tensors for Data Processing: Theory, Methods, and Applications*, Elsevier, 2021, pp. 293–340.

[24] Y. Lecun, Y. Bengio, and G. Hinton, "Deep learning," *Nature*, vol. 521, no. 7553, pp. 436–444, May 2015, doi: 10.1038/nature14539.

[25] S. K. Bahadir, "Identification and modeling of sensing capability of force sensing resistor integrated to E-textile structure," *IEEE Sensors Journal*, vol. 18, no. 23, pp. 9770–9780, Dec. 2018, doi: 10.1109/JSEN.2018.2871396.

[26] K. Sarangam, T. Appala, B. V. Vani, and A. S. Kumar, "An efficient FSR-based approach for self notifying chairs to minimize long duration sitting postures," in *2023 14th International Conference on Computing Communication and Networking Technologies*, Jul. 2023, pp. 1–5, doi: 10.1109/ICCCNT56998.2023.10306812.

[27] A. Erwin, F. Sergi, V. Chawda, and M. K. O'Malley, "Interaction control for rehabilitation robotics via a low-cost force sensing handle," in *ASME 2013 Dynamic Systems and Control Conference*, Oct. 2013, vol. 2, doi: 10.1115/DSCC2013-4073.

[28] C. Madeu, F. J. Garcia, and Y. Ye Lin, "Desarrollo de un sistema para la monitorización de contracción muscular en base a un sensor de presión en superficie [trabajo final de grado en Internet]," *Universidad politécnica de Valencia*, 2016.

[29] J. A. Flórez and A. Velásquez, "Calibration of force sensing resistors (fsr) for static and dynamic applications," in *2010 IEEE ANDESCON Conference Proceedings*, Sep. 2010, pp. 1–6, doi: 10.1109/ANDESCON.2010.5633120.

[30] W. C. Hsu, T. Sugiarto, J. W. Chen, and Y. J. Lin, "The design and application of simplified insole-based prototypes with plantar pressure measurement for fast screening of flat-foot," *Sensors (Switzerland)*, vol. 18, no. 11, p. 3617, Oct. 2018, doi: 10.3390/s18113617.

[31] V. Gracia-Ibáñez, M. Vergara, J. L. Sancho-Bru, M. C. Mora, and C. Piqueras, "Functional range of motion of the hand joints in activities of the international classification of functioning, disability and health," *Journal of Hand Therapy*, vol. 30, no. 3, pp. 337–347, Jul. 2017, doi: 10.1016/j.jht.2016.08.001.

[32] V. Gracia-Ibáñez, P. J. Rodríguez-Cervantes, V. Bayarri-Porcar, P. Granell, M. Vergara, and J. L. Sancho-Bru, "Using sensorized gloves and dimensional reduction for hand function assessment of patients with osteoarthritis," *Sensors*, vol. 21, no. 23, p. 7897, Nov. 2021, doi: 10.3390/s21237897.

[33] A. Roda-Sales, M. Vergara, J. L. Sancho-Bru, V. Gracia-Ibáñez, and N. J. Jarque-Bou, "Human hand kinematic data during feeding and cooking tasks," *Scientific Data*, vol. 6, no. 1, p. 167, Sep. 2019, doi: 10.1038/s41597-019-0175-6.

[34] N. J. Jarque-Bou, M. Vergara, J. L. Sancho-Bru, V. Gracia-Ibanez, and A. Roda-Sales, "Hand kinematics characterization while performing activities of daily living through kinematics reduction," *IEEE Transactions on Neural Systems and Rehabilitation Engineering*, vol. 28, no. 7, pp. 1556–1565, Jul. 2020, doi: 10.1109/TNSRE.2020.2998642.

[35] M. R. Cutkosky, "On grasp choice, grasp models, and the design of hands for manufacturing tasks," *IEEE Transactions on Robotics and Automation*, vol. 5, no. 3, pp. 269–279, Jun. 1989, doi: 10.1109/70.34763.

[36] O. A. M. López, A. M. López, and J. Crossa, "Fundamentals of artificial neural networks and deep learning," in *Multivariate Statistical Machine Learning Methods for Genomic Prediction*, Cham: Springer International Publishing, 2022, pp. 379–425.

[37] A. Halnaut, R. Giot, R. Bourqui, and D. Auber, "Compact visualization of DNN classification performances for interpretation and improvement," in *Explainable Deep Learning AI: Methods and Challenges*, Elsevier, 2023, pp. 35–54.

[38] N. Srivastava, G. Hinton, A. Krizhevsky, I. Sutskever, and R. Salakhutdinov, “Dropout: a simple way to prevent neural networks from overfitting,” *Journal of Machine Learning Research*, vol. 15, no. 1, pp. 1929–1958, 2014.

[39] M. Grandini, E. Bagli, and G. Visani, “Metrics for multi-class classification: an overview,” 2020, doi: 10.48550/arXiv.2008.05756.

[40] J. Hamill and K. Knutzen, *Biomechanical basis of human movement*, 3rd ed. Lippincott Williams & Wilkins, 2009.

[41] D. Falk, L. Aiello, and C. Dean, “An introduction to human evolutionary anatomy.,” *Man*, vol. 27, no. 2, p. 410, 1992, doi: 10.2307/2804064.

[42] Y. Yang, C. Fermüller, Y. Li, and Y. Aloimonos, “Grasp type revisited: a modern perspective on a classical feature for vision,” in *Proceedings of the IEEE Computer Society Conference on Computer Vision and Pattern Recognition*, Jun. 2015, vol. 07-12-June-2015, pp. 400–408, doi: 10.1109/CVPR.2015.7298637.

[43] E. Peña-Pitarch, J. F. P. Magaña, N. Ticó-Falguera, A. Al Omar, I. A. Larrión, and J. V. Costa, “Virtual human hand: grasps and fingertip deformation,” in *Advances in Intelligent Systems and Computing*, vol. 975, 2020, pp. 484–492.

[44] J. W. Lee and K. Rim, “Measurement of finger joint angles and maximum finger forces during cylinder grip activity,” *Journal of Biomedical Engineering*, vol. 13, no. 2, pp. 152–162, Mar. 1991, doi: 10.1016/0141-5425(91)90062-C.

[45] N. M. Ali, R. Besar, and N. A. A. Aziz, “A case study of microarray breast cancer classification using machine learning algorithms with grid search cross validation,” *Bulletin of Electrical Engineering and Informatics (BEEI)*, vol. 12, no. 2, pp. 1047–1054, Apr. 2023, doi: 10.11591/eei.v12i2.4838.

[46] G. N. Ahmad, H. Fatima, Shafiullah, A. S. Saidi, and Imdadullah, “Efficient medical diagnosis of human heart diseases using machine learning techniques with and without GridSearchCV,” *IEEE Access*, vol. 10, pp. 80151–80173, 2022, doi: 10.1109/ACCESS.2022.3165792.

[47] E. Cho, R. Chen, L. K. Merhi, Z. Xiao, B. Pousett, and C. Menon, “Force myography to control robotic upper extremity prostheses: a feasibility study,” *Frontiers in Bioengineering and Biotechnology*, vol. 4, Mar. 2016, doi: 10.3389/fbioe.2016.00018.

[48] H. S. Nam, W. H. Lee, H. G. Seo, Y. J. Kim, M. S. Bang, and S. Kim, “Inertial measurement unit based upper extremity motion characterization for action research arm test and activities of daily living,” *Sensors (Switzerland)*, vol. 19, no. 8, p. 1782, Apr. 2019, doi: 10.3390/s19081782.

[49] B. O’Flynn, J. Torres, J. Connolly, J. Condell, K. Curran, and P. Gardiner, “Novel smart sensor glove for arthritis rehabiliation,” in *2013 IEEE International Conference on Body Sensor Networks*, May 2013, pp. 1–6, doi: 10.1109/bsn.2013.6575529.

BIOGRAPHIES OF AUTHORS

Jesus Fernando Padilla-Magaña received the Ph.D. degree in the program of automatics, robotics and vision from the Polytechnic University of Catalonia in Barcelona, Spain. Currently, he is full time Professor at the Polytechnic University of Uruapan, Mexico in the department of manufacturing technologies engineering. Currently he has the distinction as National Researcher LEVEL I granted by CONAHCYT in the National System of Researchers of Mexico. His research is focused on the medical rehabilitation, analysis of human motion, wearable sensors, development of medical devices, and the development of algorithms in the area of artificial intelligence (machine learning and deep learning). He can be contacted at email: fe.padilla@upu.edu.mx.

Isahi Sanchez-Suarez received the Ph.D. degree from the Universidad Michoacana de San Nicolás de Hidalgo at the Institute of Physics and Mathematics. He did a postdoctoral stay at the Mathematics Department UNAM in Morelia, Michoacán. Currently he has the distinction as National Researcher LEVEL II granted by CONAHCYT in the National System of Researchers of Mexico. Currently attached to the Polytechnic University of Uruapan, Michoacan as full time Professor C, from 2016 to date. He can be contacted at email: i.sanchez@upu.edu.mx.

Esteban Peña-Pitarch received the Ph.D. degree from the Polytechnic University of Catalonia in Barcelona, Spain. He has carried out his teaching work at the Technical College of Manresa (EPSEM), since 1988 and belongs to the department of mechanical engineering. He collaborates with the Institute of Industrial and Control Engineering (IOC), UPC, since 2008, in the robotics division. His research is focused on rehabilitation and simulation of stroke survivors, the creation of medical devices and the application of kinematics and dynamics to the human body by way of mathematical tools used in robotics. He can be contacted at email: esteban.pena@upc.edu.